Air-Trapping on Biocompatible Nanopatterns

ARTICLE *in* LANGMUIR · JANUARY 2007

Impact Factor: 4.46 · DOI: 10.1021/la061611t · Source: PubMed

Air-Trapping on Biocompatible Nanopatterns

Elena Martines,[†] Kris Seunarine,[‡] Hywel Morgan,[§] Nikolaj Gadegaard,[‡] Chris D. W. Wilkinson,[‡] and Mathis O. Riehle*,[†]

Centre for Cell Engineering, IBLS, University of Glasgow, Glasgow, G12 8QQ, UK, Department of Electronics and Electrical Engineering, University of Glasgow, Glasgow, G12 8QQ, UK, and School of Electronics and Computer Science, University of Southampton, S017 1BJ, UK

Received June 5, 2006. In Final Form: September 24, 2006

The occurrence of air-trapping inside poly-ϵ-caprolactone nanopits was investigated by measuring the contact angles of water droplets on a set of defined nanotopographies. It is shown that the advancing angles follow the Cassie−Baxter theory, thus revealing the presence of air bubbles inside the biodegradable nanopatterns. The importance of these observations for the definition of hydrophilicity/hydrophobicity and in the context of in vitro cell behavior is discussed.

Introduction

The wettability of solid surfaces is still raising great interest, not only because it can be used for potential applications, e.g. in the development of self-cleaning surfaces or in wettability-driven microfluidics,[1,2] but also because it is related to the biocompatibility of solid surfaces.[3] It has been shown that a surface made of a biodegradable polymer (poly-ϵ-caprolactone) can inhibit the adhesion of fibroblastic cells when the surface is patterned with nanopits (diameter 216 nm, depth 100 nm, pitch 300 nm).[4] Since nanostructured surfaces can trap air between asperities,[5] the presence of air bubbles might be the underlying reason for changes in cell behavior on nanotopographies.

The occurrence of air-trapping on a rough surface depends on both the topography and the surface energy of a substrate. The surface energy of a sample will determine if a drop of a given liquid, when deposited on it, will assume a quasispherical shape (indicating that the liquid is being repelled by the surface) or if it spreads and wets the substrate. Roughening a surface enhances its repellent or wetting properties.[6] Different theories have been formulated to explain the effect of surface roughness on wettability. Wenzel's model[7] predicts that both hydrophobicity ($\theta_Y > 90°$) and hydrophilicity ($\theta_Y < 90°$) are reinforced by the roughness, by assuming that the liquid penetrates between the surface topography (Figure 1a). The contact angle on the rough surface is modified by the roughness factor according to

$$\cos \theta_W = r \cos \theta_Y \quad (1)$$

where θ_W is the apparent contact angle on the rough surface, θ_Y is the ideal contact angle of water (Young's angle) on a smooth surface of identical chemistry, and r is the roughness factor, which is defined as the ratio of actual surface area over the projected surface area.

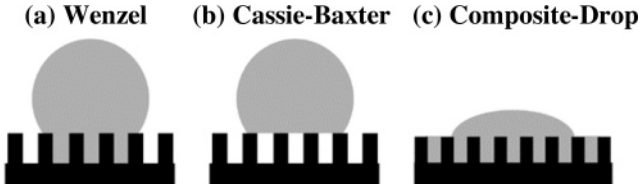

Figure 1. Schematic of the possible behaviors of a drop on a nanostructured interface according to three accepted theoretical models.

The Cassie−Baxter model on the other hand predicts that hydrophobicity is enhanced because air is trapped inside the topography[8] and applies only to hydrophobic surfaces. The drop sits on a composite surface composed of a mix of air and solid (Figure 1b). The Cassie−Baxter contact angle on the rough surface is given by

$$\cos \theta_{CB} = r_f f \cos \theta_Y + (1 - f)\cos \theta_{air} \quad (2)$$

where θ_{CB} is the apparent contact angle on a rough surface, r_f is the roughness factor of the wetted area, and f is the area fraction of the projected wet area. The product $r_f f$ is often called the solid fraction ϕ_S. Since the water contact angle on air is $\cos \theta_{air} = -1$, the final expression of the Cassie−Baxter angle is

$$\cos \theta_{CB} = r_f f \cos \theta_Y + f - 1 \quad (3)$$

For hydrophilic surfaces another model, besides Wenzel's, has been formulated; it is the "hemi-wicking" or composite-drop model,[9] where the drop is assumed to be sitting on a surface of mixed state, composed of solid and water in different ratios (Figure 1c):

$$\cos \theta_{comp} = 1 + \phi_S(\cos \theta_Y - 1) \quad (4)$$

All three of these models (for both hydrophobic and hydrophilic rough surfaces) were originally formulated for static drops at equilibrium. However, it has been shown that the low-rate advancing angles and static angles are essentially identical,[10] so that all the models are applicable to advancing angles.

* Corresponding author. Tel: 0044-141-3302931. Fax: 0044-141-3303730. E-mail: m.riehle@bio.gla.ac.uk.
[†] Centre for Cell Engineering, University of Glasgow.
[‡] Department of Electronics and Electrical Engineering, University of Glasgow.
[§] University of Southampton.

(1) Blossey, R. *Nat. Mater.* **2003**, *2*, 301−306.
(2) Grunze, M. *Science* **1999**, *283*, 41−45.
(3) Vogler, E. A. *Adv. Colloid Interface Sci.* **1998**, *74*, 69−117.
(4) Gallagher, J. O.; McGhee, K. F.; Wilkinson, C. D. W.; Riehle, M. O. *IEEE Trans. Nanobiosci.* **2002**, *1*.
(5) Martines, E.; Seunarine, K.; Morgan, H.; Gadegaard, N.; Wilkinson, C. D. W.; Riehle, M. *Nano Lett.* **2005**, *5*, 2097−2103.
(6) Bico, J.; Thiele, U.; Quere, D. *Colloids Surf. A* **2002**, *206*, 41−46.
(7) Wenzel, R. N. *Ind. Eng. Chem.* **1936**, *28*, 988−994.
(8) Cassie, A. B. D.; Baxter, S. *Trans. Faraday Soc.* **1944**, *40*, 546.
(9) Quere, D. *Physica A* **2002**, *313*, 32−46.
(10) Kwok, D. Y.; Lin, R.; Neumann, A. W. *Colloids Surf. A* **1996**, *116*, 63−77.

10.1021/la061611t CCC: $33.50
Published on Web 11/07/2006

Since it has been shown that the Wenzel, Cassie−Baxter, and composite-drop laws can successfully predict contact angles on nanopatterned surfaces,[5] it is possible to infer the presence of trapped air in a surface with nanotopography by measuring the advancing angle of a liquid drop deposited on it. However, the existence and stability of nanobubbles (or more precisely, nanocavities), even on hydrophobic surfaces, are controversial.[11] Although the occurrence of nanobubbles has been suspected to influence colloidal stability[12] and cavitation probability,[13] their existence is hard to reconcile with thermodynamics. Such small cavities should rapidly dissolve because of their high internal pressure. Nevertheless, Tyrrell et al.[14] claimed that nanobubbles could be AFM-imaged at a time interval of 10−20 min. Moreover, it has been suggested that this phenomenon is increased by submicrometric roughness.[15]

It has recently been observed that surfaces that exhibit low hydrophilicity ($\theta_Y \approx 70°$) can, when nanopatterned, induce Cassie−Baxter behavior in water droplets.[16] This behavior indicates that air-trapping can occur even on materials that are not defined as strictly "hydrophobic", i.e., where the ideal contact angle $\theta_Y < 90°$.[17] In this study, ordered arrays of silicon nanopillars have been fabricated and rendered hydrophobic by surface silanization. The patterns were replicated by embossing directly into sheets of poly-ϵ-caprolactone (PCL), which is a weakly hydrophilic ($\theta_Y = 77°$) biodegradable polymer. Both the advancing and receding contact angles of water droplets were measured on the PCL nanopitted replicas. The nanopit dimensions of each sample were measured and the experimental advancing angles were compared to the analytical models. The presence of air-bubbles within the PCL nanotopographies could then be determined.

Materials and Methods

Fabrication of PCL Nanopatterns. The fabrication and hydrophobisation of silicon nanopillars has been detailed elsewhere.[5] Briefly, the pillars were fabricated in the master using electron beam lithography of silicon wafers (4 in., ·100⟩, p-doped, 525 ± 50 μm thick) to pattern an area of 1 cm × 1 cm. The masters were diced and hydrophobized with octadecyltricholorosilane (OTS, Sigma). Poly-ϵ-caprolactone (PCL) pellets were purchased from Sigma. Sheets of polymer (thickness ≈ 0.5 mm) were prepared by placing pellets on a square between two glass plates. The plates were clamped and the assembly was kept for more than 3 h at 70 °C in an oven. At this temperature the PCL melted and formed a sheet. On cooling, the polymer was easily separated from the glass and the sheet was cut into squares (0.7 cm × 0.7 cm). The silicon masters were placed on a hot plate at 85 °C, and a square of PCL was placed on top of the patterned area. When the polymer had melted, a glass slide was pressed on it for a few seconds (by hand), producing an imprint of the nanopattern from the Si master into the PCL. The sandwich (master/PCL/slide) was immediately transferred into RO water for cooling, after which the polymer was easily detached from both surfaces. PCL replicas were blow-dried with N_2.

Scanning Electron Microscopy. The silicon surfaces and the PCL replicas were imaged with a Hitachi S4700. After contact angle measurements, individual samples were cleaved and their SEM profiles were used to measure the dimensions of the nanotopographies (silicon nanopillars and PCL nanopits) with ImageJ.[18] The PCL replicas were imaged after sputter-coating with 20 nm gold−palladium (Emscope, Ashford, UK). To cleave the PCL nanopits, the replicas were plunged in liquid nitrogen and then split with a cooled scalpel from the backside. After sputter-coating and imaging, the SEM images of the profiles were analyzed to determine the exact dimensions of the embossed nanopits.

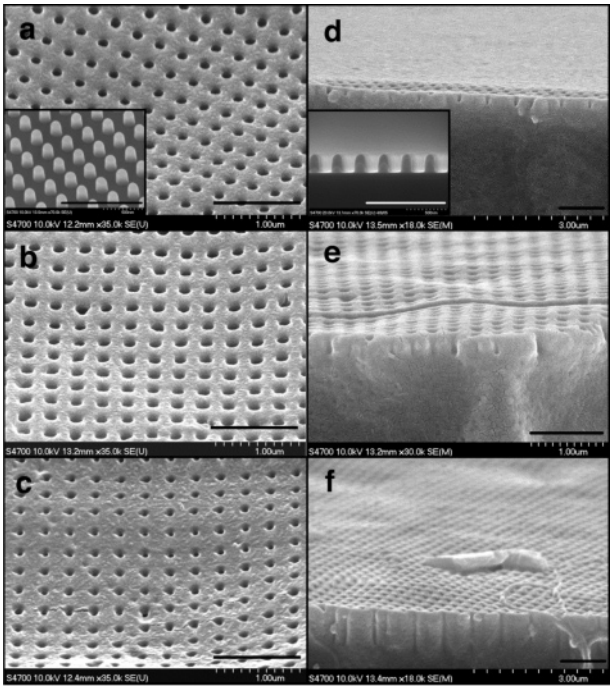

Figure 2. SEM images of PCL replicas. (a) P22r; the inset shows the source silicon master; (b) P21r; (c) P12r; (d) profile of P22r; the inset shows the profile of the source silicon master; (e) profile of P21r; (f) profile of P12r. Tilt: (a−c) 45°, (d−f) 90°. Bars: 1 μm.

Atomic Force Microscopy. A total of 10 flat PCL samples were scanned across 1 μm × 1 μm areas (at least three images/sample) with an AFM (NanoScope III, Digital Instruments) in tapping mode. The root mean square (rms) roughness of the polymer was then determined.

Dynamic Contact Angle Measurements. Images of the advancing and receding contact angles of filtered Milli-Q water were captured at a rate of two images per second with a long-distance objective connected to a CCD camera and analyzed with the FTÅ200 software (v2.0, First Ten Ångstroms). Water drops (5 μL) were deposited on the surface and then withdrawn through a 30-gauge flat-tipped needle, at a rate of 0.25 μL/s. At this rate, the advancing angle was seen to be identical to the static angle, confirming the quasistaticity of the dynamic regime. The values reported are averages of at least five measurements made on different areas of the sample. All measurements were performed at room temperature on a vibration-free platform.

Results

Nanopatterns. SEM images of the PCL nanopits are shown in Figure 2. The different patterns were named after the solid fraction percentage of the silicon master from which they were embossed (e.g. P22r was replicated from silicon master P22). The masters were named after the solid fraction ϕ_S: For instance, P22 indicates a pillared sample where the tops of the pillars represent 22% of the projected surface area. Table 1shows the dimensions of the silicon nanopatterns (base diameter *d*, height *h*, center-to-center pitch *l*), and the corresponding PCL replicas.

(11) Mao, M.; Zhang, J.; Yoon, R.; Ducker, W. A. *Langmuir* **2004**, *20*, 1843−1849.
(12) Snoswell, D. R. E.; Duan, J.; Fornasiero, D.; Ralston, J. *J. Phys. Chem. B* **2003**, *107*, 2986−2994.
(13) Bunkin, N. F.; Kiseleva, O. A.; Lobeyev, A. V.; Movchan, T. G.; Ninham, B. W.; Vinogradova, O. I. *Langmuir* **1997**, *13*, 3024−3028.
(14) Tyrrell, J. W. G.; Attard, P. *Phys. Rev. Lett.* **2001**, *87*, 176104−1.
(15) Ryan, W. L.; Hemmingsen, E. A. *J. Colloid Interface Sci.* **1998**, *197*, 101−107.
(16) Abdelsalam, M. E.; Bartlett, P. N.; Kelf, T.; Baumberg, J. *Langmuir* **2005**, *21*, 1753−1757.
(17) Herminghaus, S. *Europhys. Lett.* **2000**, *52*, 165.
(18) Rasband, W. S.; ImageJ, U. S. National Institutes of Health: Betheda, MD, 1997−2006; http://rsb.info.nih.gov/ij/.

Table 1. Dimensions of the Silicon Nanopatterns and the Corresponding PCL Replicas[a]

	P22	P22r	P21	P21r	P12	P12r
d (nm)	157 ± 5 (7)	130 ± 9 (97)	156 ± 5 (8)	147 ± 8 (125)	117 ± 5 (16)	88 ± 11 (92)
h (nm)	239 ± 5 (8)	214 ± 23 (50)	286 ± 5 (8)	275 ± 18 (46)	792 ± 5 (16)	757 ± 57 (20)
l (nm)	300	300	300	300	300	300

[a] Values are mean ± one standard deviation. All dimensions were measured with ImageJ, except the pitch *l* that was assumed to be constant. *h* indicates the maximum distance from the base to the top. In parentheses are the total number of averaged values (*n*).

Table 2. Experimental Advancing (θ_{adv}) and Receding Angles (θ_{rec}) of Water (5 μL Drop) on PCL Replicas[a]

	flat	P22r	P21r	P12r
θ_{adv} (deg)	77 ± 2^a	95 ± 3^c	95 ± 1^e	84 ± 2^g
θ_{rec} (deg)	56 ± 2^b	44 ± 2^d	28 ± 3^f	37 ± 10^h

[a] Results are mean ± one standard deviation, with the superscripted letter denoting the total number of averaged values: (a) 211, (b) 129, (c) 157, (d) 70, (e) 95, (f) 27, (g) 68, (h) 37.

The rms roughness of flat PCL as measured by AFM was 5.3 ± 1 nm.

Contact Angles. The experimental advancing and receding angles (θ_{adv} and θ_{rec}) for the PCL replicas are shown in Table 2. The Young's angle for these substrates was taken as the advancing angle measured on flat PCL sheets ($\theta_Y = 77° \pm 2°$).

Discussion

The advancing angles measured on the PCL nanopits are plotted in Figure 3, together with the angles predicted by the Cassie−Baxter, composite-drop, and Wenzel models for cylindrical pits.

The advancing angles of water on the nanopitted PCL replicas are discussed within the framework of Patankar's criterion for hydrophobic surfaces,[19] even though this material could be classified as weakly hydrophilic ($\theta_Y = 77° < 90°$). The reason for this choice is apparent from Figure 3: the experimental advancing angles of samples P22r, P21r, and P12r are in agreement with the Cassie−Baxter curve for cylindrical nanopits (Figure 3a), even more so if the dimensions of the nanopits are assumed to be the exact negative of the master dimensions (Figure 3b). This could be due to several reasons. On one hand, the dimensions of the replicated nanopits might be closer to the dimensions of the nanopillared masters, and the measurements could be biased by PCL deformation during the cleaving, or during SEM examination. On the other hand, because of the natural roughness of PCL, the nanopits could actually be the larger part of a double-scale structure, which is known to affect the contact angle of rough surfaces.[20,21]

This Cassie−Baxter state, which suggests that air is trapped in the nanopits, is constantly metastable, since all the composite-drop and Wenzel curves in this case correspond to a lower energy configuration. Moreover, it is unclear from the receding angles (see Table 2) if, on retracting, the drops undergo a transition to the Wenzel state, since the hysteresis ($\theta_{adv} - \theta_{rec}$) is quite high.[22] Nevertheless, these results confirm the hypothesis of Herminghaus,[17] who claimed that given the appropriate steepness of the pits, a free liquid surface can be formed, resulting in air-trapping (i.e. increased hydrophobicity) even on surfaces with $\theta_Y < 90°$. Abdelsalam et al.[16] patterned a gold surface ($\theta_Y \approx 70°$) with 500-nm close-packed hemispherical pits, thus inducing a Cassie−Baxter behavior in water droplets. Even though they explain the phenomenon by a particular curvature of the liquid−vapor interface on the pores, it is interesting to note that the Young's angle on their gold substrates is comparable to the contact angle of PCL (77°). This calls for consideration of the definition of hydrophilicity and hydrophobicity. If the defining criterion is the contact angle θ, then $\theta_{hydrophilic} < 90°$ and $\theta_{hydrophobic} > 90°$; however, it has been pointed out[3,23] that if the defining criterion is the structural force between surfaces, the hydrophobic/hydrophilic boundary should correspond to an angle of 62°−65°, which is consistent with the observations reported here. This suggests that the modeling approaches for hydrophilic surfaces, expecting a composite-drop or Wenzel trend when $\theta_Y < 90°$, will fail with substrates showing $65° < \theta_Y < 90°$, since air-trapping, although metastable, is possible in this case.

The existence of submicrometric air pockets at a solid−liquid interface is highly controversial.[11] The stability of nanobubbles,

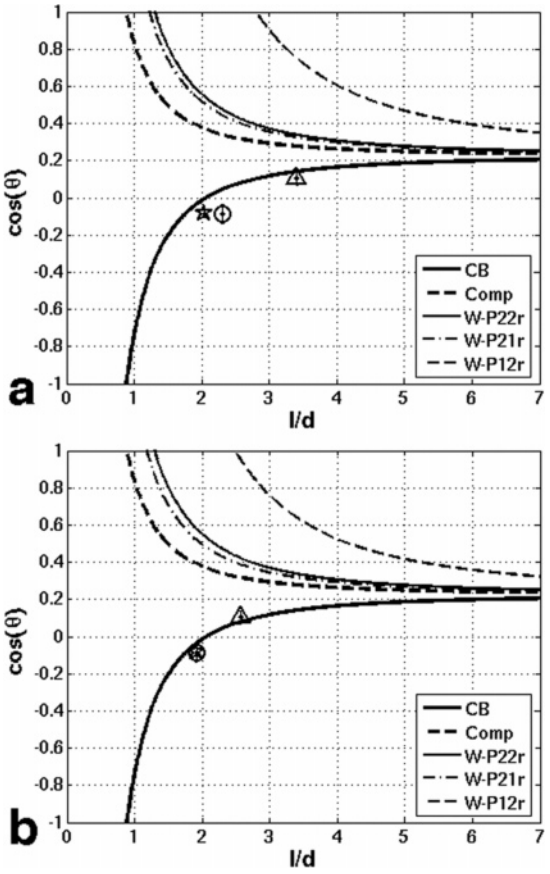

Figure 3. Plot of the apparent advancing angles of a 5 μL drop of water on PCL replicas as a function of structure geometry. (a) The nanopit dimensions were directly measured using ImageJ from the SEM images. (b) The nanopit dimensions are assumed to be the exact negative of the corresponding silicon masters. The Cassie−Baxter (CB), composite-drop (Comp), and Wenzel (W-) curves for cylindrical pits are shown. Individual points indicate experimental data: (○) P22r, (☆) P21r, (Δ) P12r.

(19) Patankar, N. A. *Langmuir* **2003**, *19*, 1249−1253.
(20) Shirtcliffe, N. J.; McHale, G.; Newton, M. I.; Chabrol, G.; Perry, C. C. *Adv. Mater.* **2004**, *16*, 1929−1932.
(21) Patankar, N. A. *Langmuir* **2004**, *20*, 8209−8213.
(22) Lafuma, A.; Quere, D. *Nature Mater.* **2003**, *2*, 457−460.
(23) Hayashi, T.; Pertsin, A. J.; Grunze, M. *J. Chem. Phys.* **2002**, *117*, 6271−6280.

or more exactly nanocavities, on surfaces is related to their size, according to Laplace equation

$$P_{int} - P_{ext} = 2\gamma/r \quad (5)$$

where P_{int} is the internal pressure in the cavity, P_{ext} is the external pressure, γ is the surface tension, and r is the radius of the cavity. According to eq 5, the internal pressure of a bubble with a radius of 50 nm in water is 30 atm, meaning that the gas should rapidly dissolve in water. However, nanocavities have been imaged and claimed to be stable still after 10−20 min.[14]

Investigating the occurrence and stability of nanobubbles of air on a biocompatible surface is extremely relevant to the field of tissue engineering. Cell adhesion to a surface will be inevitably affected by the presence of air pockets; depending on the surface topography and on the stability of the bubbles, the surface area available for initial cell attachment and possibly long-term focal contact formation would be reduced. Therefore, further investigation of the stability of nanocavities is needed, and the presence of trapped air on the surface should be determined when culturing biological cells in vitro on nanopatterned substrates.

Conclusion

Regular nanopillars were fabricated in silicon wafers and the patterns replicated in PCL. The behavior of water droplets on the nanopitted replicas was evaluated by contact angle measurements. The PCL nanopits exhibited a Cassie−Baxter behavior, despite the ideal contact angle on PCL being less than 90°. These results, besides proving that air-trapping can occur on such "hydrophilic" surfaces, are in agreement with previous work[16,17] and strongly support the consideration that the hydrophobic/hydrophilic boundary contact angle is not 90°, but rather between 62° and 90°.[3,23] The occurrence of air-trapping on a nanopatterned biomaterial could influence the results of in vitro cell culture, and this factor should be considered when assessing the biocompatibility of a nanostructured surface.

Acknowledgment. Many thanks to F. Madani, V. Koutsos, M. Robertson, and O. Meredith. The partial support by the EC-funded projects NaPa (Contract no. NMP4-CT-2003-500120) and Nanocues (FP6-NMP-2002-3.4.1.2-1) is gratefully acknowledged. The content of this work is the sole responsibility of the authors.

LA061611T